Journal of Engineering Sciences
Vol 11, Issue 4 ,April/2020
ISSN NO:0377-9254

# ANALYSIS OF RESIDUAL STRESSES IN A BUTT WELD USING ANSYS SOFTWARE

**Y.UDAY KUMAR[1], N.BHASKAR[2], P.MALLIKARJUNA[3]**
[1]Assistant Professor, Dept of Mechanical Engineering, AITK, Kadapa, AP, India.
[2]Assistant Professor, Dept of Mechanical Engineering, AITK, Kadapa, AP, India.
[3]Assistant Professor, Dept of Mechanical Engineering, AITK, Kadapa, AP, India.

**Abstract—**Low carbon steels are prone to distortion and cracks due to residual stresses induced during welding. This project gives the information about the residual stresses induced in a butt weld joint due to welding. Experimentation was carried out on a plate made of low carbon steel having dimensions 0.115 x 0.048 x 0.006 meters. The type of welding chosen is Manual Metal Arc Welding (MMAW). Single pass welding was carried out. Experimental values calculated were taken as input for the analysis in ANSYS software. A model was generated in ANSYS 9.0 (A general purpose FEA software) using SOLID BRICK 8 NODE 70 (3D solid element with temperature dof) and PLANE 55 (A 2D Solid Element with 4 nodes), as per the dimensions of the plate taken for the experimentation. A refined mesh is made based on the convergency criteria and the analysis is performed to estimate the temperature distribution. Firstly a transient thermal analysis was carried out by giving heat flux as the time varying input to estimate the temperature variation. The non-linear material properties are fed for the heat transfer solution. Then coupled field analysis is carried out to get the residual stresses by coupling thermal analysis to static analysis. The variation of the temperature with time, and residual stresses are obtained. The variation of these are reported and discussed.

## I. INTRODUCTION

The basic idea in the Finite Element Method is to find the solution of complicated problems with relatively easy way. The Finite Element Method has been a powerful tool for the numerical solution of a wide range of engineering problems. Applications range from deformation and stress analysis of automotive, aircraft, building, defense, and missile and bridge structures to the field of analysis of dynamics, stability, fracture mechanics, heat flux, fluid flow, magnetic flux, seepage, and other flow problems. With the advances in computer technology and CAD systems, complex problems can be modeled with relative ease. Several alternate configurations can be tried out on a computer before the first prototype is built. The basics in engineering field are must to idealize the given structure for the required behaviour. In the Finite Element Method, the solution region is considered as many small, interconnected sub regions called Finite elements. Most often it is not possible to ascertain the behaviour of complex continuous systems without some form of approximations. For simple members like uniform beams, plates etc., classical solutions can be sought by forming differential and/or integral equations through structures like machine tool frames, pressure vessels, automobile bodies, ships, aircraft structures, domes etc., need some approximate treatment to arrive at their behaviour, be it static deformation, dynamic properties or heat conducting property. Indeed these are continuous systems with their mass and elasticity being continuously distributed. The classical differential equation solution approach leads to intractability. To overcome this, engineers and mathematicians have from time to time proposed complex structures, which are defined using a finite number of well-defined components. Such systems are then regarded as discrete systems.

## II. MODELING OF BUTT WELD USING FEA

The process of forming a butt weld that joins two steel plates was simulated. The overall dimensions adopted are 0.115 x 0.048 x 0.006 meters. The welding procedure is modeled as a single pass in this analysis. The weldment was assumed to be symmetric so that only one half of the model was analyzed. No penetration and overfill of the weldment were considered.

The FE analysis was carried out in two steps. A non-linear transient thermal analysis was conducted first to obtain the global temperature history generated during the welding process. A stress analysis was then developed with the temperatures obtained from the thermal analysis used as loading to the stress model. The general purpose FE package ANSYS was used for both thermal and stress analysis performed sequentially. The mesh used in the stress analysis was identical to that in the thermal analysis.

**A. BASIC SYMMETRICAL MODEL OF A WELD PLATE**

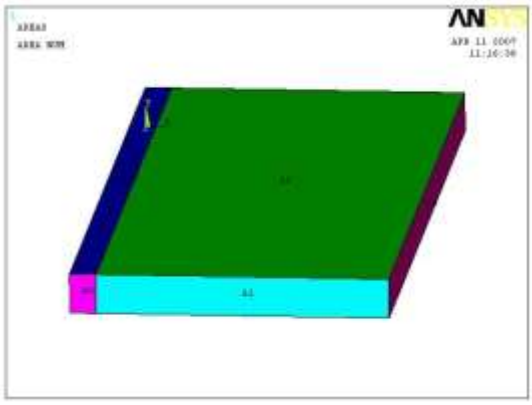

Fig.1: symmetric model showing the areas

**1. 2D MESH MODEL**

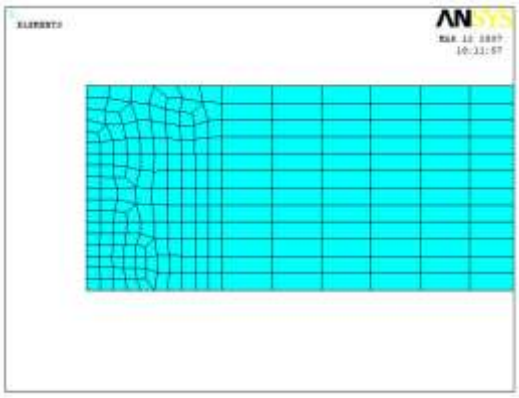

Fig.2: 2D Mesh model of the weld plate.

**2. 3D MESH MODEL**

Fig.3: 3D Mesh model

**B. PROBLEM DEFINITION:**

A Finite Element (FE) simulation of the welding process yielding the welding-induced residual stresses in a butt-welded plate is presented. In fusion welding, a weldment is locally heated by the welding heat source. Due to the non-uniform temperature distribution during the thermal cycle, incompatible strains lead to thermal stresses. These incompatible strains due to dimensional changes associated with solidification of the weld metal (WM), metallurgical transformations, and plastic deformation, are the sources of residual stresses and distortion. Welding-induced residual stresses and distortion can play a very important role in the reliable design of welded joints and welded structures.Here, a finite element simulation of the welding process yielding the welding-induced residual stresses in a butt-welded plate is presented.

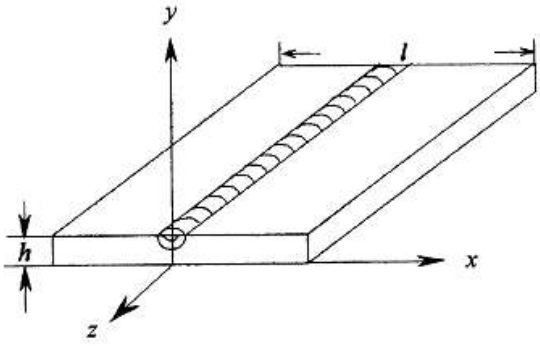


Fig.4: Schematic diagram of welding test plate

**C. MATERIAL USED:**

Carbon steel, also called plain carbon steel, is a metal alloy, a combination of two elements, iron and carbon, where other elements are present in quantities too small to affect the properties. The only other alloying elements allowed in plain-carbon steel are: manganese (1.65% max), silicon (0.60% max), and copper (0.60% max). Steel with low carbon content has the same properties as iron, soft but easily formed. As carbon content rises the metal becomes harder and stronger but less ductile and more difficult to weld. Higher carbon content lowers steel's melting point and its temperature resistance in general.

**LOW CARBON STEEL:**

Low carbon steel approximately contains 0.05% - 0.29% carbon content (e.g. AISI 1018 steel). Mild steel has a relatively low tensile strength, but it is cheap and malleable; surface hardness can be increased through carburizing.It is a hypo eutectoid steel containing 0.2 percent carbon. In the austenitic range this alloy consists of a uniform interstitial solid solution. Each grain contains 0.2 percent carbon dissolved in spaces of the f.c.c iron lattice structure. It contains 75% proeutectoid ferrite and 25% pearlite. The pearlite present her is a fine fingerprint mixture, which can be seen clearly at higher magnification

**D. MATERIAL PROPERTIES**

Several different material have been used in structures where welding is involved, with low carbon steel being the most common. The weldment material properties employed in this work were mild steel, which were taken from Brown and Song (1992).

Two sets of temperature dependent material properties (Table 1) were needed in the analyses. The modulus of elasticity is a measure of the stiffness of a material. A higher modulus material is more likely to resist distortion. The amount of expansion or contraction of a metal will undergo during a heating or a cooling cycle depends on the coefficient of thermal expansion. Thermal conductivity gives a measure of the ease of heat flow through a material.

Table:1 Temperature- Dependent Material Properties for both Steel Plate and Weld.

| T (Celsius) | E (MPa) | N | $\alpha_d$ ($10^{-6}$/°C) | K (W/m °K) | C (J/Kg °K) |
|---|---|---|---|---|---|
| 0 | 314 | 0.2786 | 10 | 51.9 | 450 |
| 100 | 349 | 0.3095 | 11 | 51.1 | 499.2 |
| 300 | 440 | 0.331 | 12 | 46.1 | 565.5 |
| 450 | 460 | 0.338 | 13 | 41.05 | 630.5 |
| 550 | 410 | 0.3575 | 14 | 37.5 | 705.5 |
| 600 | 330 | 0.3738 | 14 | 35.6 | 773.3 |
| 720 | 58.8 | 0.3738 | 14 | 30.64 | 1080.4 |
| 800 | 58.8 | 0.4238 | 14 | 26 | 931 |
| 1450 | 1.29 | 0.4738 | 15 | 29.45 | 437.93 |
| 1510 | 1.0 | 0.499 | 15 | 29.7 | 400 |
| 1580 | 0.01 | 0.499 | 15 | 29.7 | 735.25 |
| 5000 | 0.01 | 0.499 | 15.5 | 42.2 | 400 |

## E. ELEMENT DESCRIPTION

### PLANE 55:

PLANE55 can be used as a plane element or as an axisymmetric ring element with a 2-D thermal conduction capability. The element has four nodes with a single degree of freedom, temperature, at each node. The element is applicable to a 2-D, steady state or transient thermal analysis. If the model containing the temperature element is also to be analyzed structurally, the element should be replaced by an equivalent structural element (such as PLANE42).

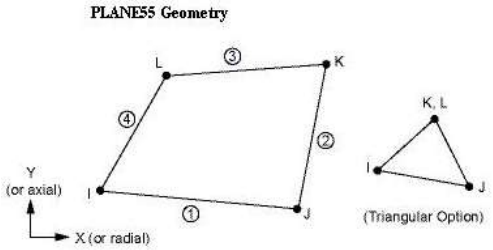


Fig.5: Plane 55 Geometry

### SOLID 70:

SOLID70 has a 3-D thermal conduction capability. The element has eight nodes with a single degree of freedom, temperature, at each node. The element is applicable to a 3-D, steady-state or transient thermal analysis. The element also can compensate for mass transport heat flow from a constant velocity field. If the model containing the conducting solid element is also to be analyzed structurally, the element should be replaced by an equivalent structural element (such as SOLID45).

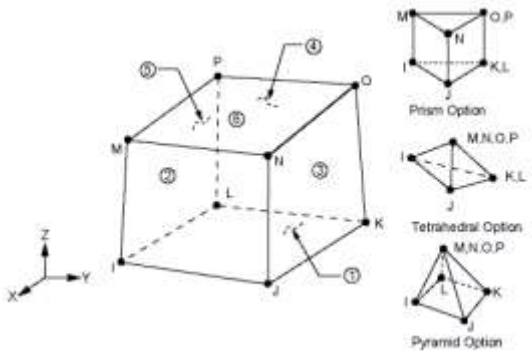


Fig.6: SOLID70 Geometry

The geometry, node locations, and the coordinate system for this element are shown in Figure "SOLID70 Geometry". The element is defined by eight nodes and the orthotropic material properties. A prism-shaped element, a tetrahedral-shaped element, and a pyramid-shaped element may also be formed as shown in Figure "SOLID70 Geometry". Orthotropic material directions correspond to the element coordinate directions.

Element loads are described in Node and Element Loads. Convection or heat flux (but not both) and radiation may be input as surface loads at the element faces as shown by the circled numbers on Figure "SOLID70 Geometry".

### F. THERMAL LOADING:

The input value i.e. the thermal loading during thermal analysis is given according to the graph shown in the figure below.

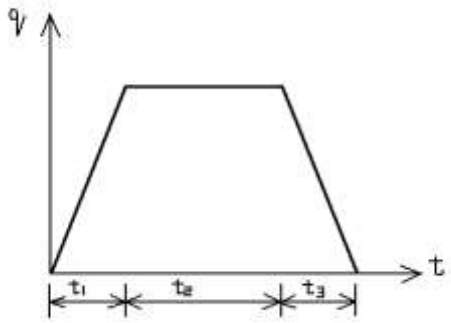


Fig.7: Ramp heat function

Time is plotted on the X-axis and the heat flux is plotted in the Y-axis. The graph begins from 0 seconds and is considered up to 200 seconds. Ramp input is given for the first 10 seconds. Step input is given up to 12 seconds. Ramp input is again given up to 200 seconds. This is because the value of heat input first increases gradually, when welding is started, until it reaches a certain value. It then remains stable for a very less amount of time and then the heat decreases gradually till the temperature of the plate reaches the value of room

temperature.
The amount of heat input was found as the product of arc efficiency, voltage, and current, which were taken equal to 0.92, 66 V and 75 A, respectively in this analysis.
**The maximum value of heat flux calculated is 8.8 x 10^6 J/m2.**
In the thermal analysis, the heat input was in three load steps corresponding to t1- t3 as shown in the figure. The nodal temperature solutions obtained from the thermal analysis were read as loading into the stress analysis. In order to capture used, the greater the computational time and the larger the store space required. The residual stresses induced due to the heating and cooling cycle, the temperature history had to be read at a sufficiently large number of time points. However, the greater the number of thermal solution steps.

**G. BOUNDARY CONDITIONS:**
**For thermal analysis:**
In a symmetrical model, convection is given on the areas as shown in figure.
The area of one plate, which is in contact with the other plate in a butt joint, is assumed to be insulated i.e., the heat flow across this area is zero.
The insulation is applied by selecting the corresponding nodes.
The value of the convective film coefficient is 0.008 W/m2-ºC

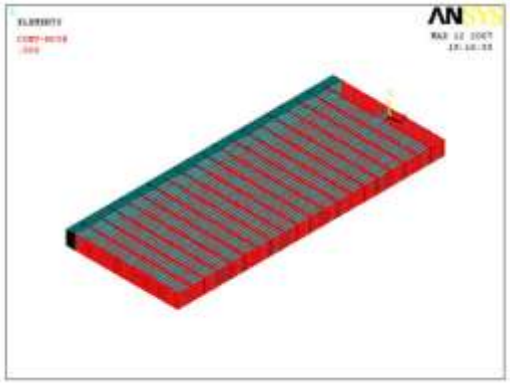

Fig.8: Thermal Boundary Conditions Applied To the Plate

**For static analysis:**
After switching from thermal analysis to static analysis, the boundary conditions assumed should be applied. In this model it is assumed that the area, as shown in figure, is constrained in all directions. That is, all degree of freedom is zero.

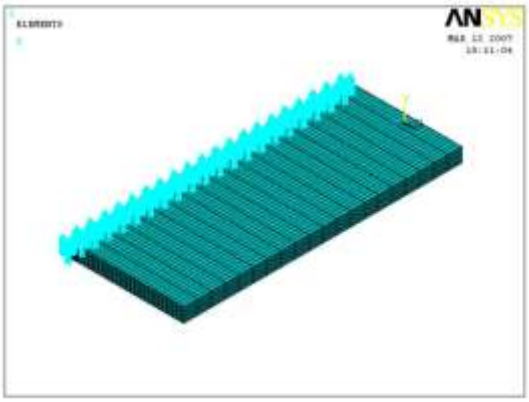

Fig.9: Boundary Conditions Applied To the Plate in Static Analysis

**Heat Transfer Analysis**
The first part of the finite element simulation of arc welding is heat transfer analysis. In the finite element formulation, this equation can be written for each element as follows
$[C(T)]\{\dot{T}\} + [K(T)]\{T\} = \{Q(T)\}$
This analysis requires an integration of the heat conduction equation with respect to time. The Crank – Nicholson/Euler theta integration method is applied to solve these system equations. This element type has a three-dimensional thermal conduction capability. The heat input from the welding electrode was modeled by using heat flux as the input for the heat transfer from the rod to the work piece. This heat flux is based on the welder setting and the efficiency of the arc.
$Q = \eta VI$

**Mechanical Analysis**
To evaluate the distortion and residual stress distribution the heat transfer analysis was performed first in order to find nodal temperatures as a function of time. Then in the second part of the analyses, a non-linear structural analysis was carried using the temperature distributions, which were obtained from the heat transfer analysis.

## III. RESULTS

Based on the results from benchmark analyses and parametric studies, the simplified modeling process for simulating welding-induced residual stresses using a general-purpose FE package described here is reliable and instructive. The main features of the simulation are:
1. A 2-D plain strain model
2. Use symmetrical feature of the model to reduce the program running time and space required
3. Simulating the 3-D effect of the arc traveling by applying a ramped heat input function. Adopting uncoupled thermal and stress analyses, the temperature history results are read from the thermal analysis as loading to the stress analysis.

The thermal analysis should be transient to trace the rapid change of temperature with time while a static analysis can be adopted for the stress analysis. However, a significant number of time points, at which the temperature results are to be read into the stress analysis, should be defined to capture the temperature gradient and give accurate residual stress results using the load steps option.

4. Radiation and latent heat from phase transformation can be ignored to simplify the modeling procedure.

1. T max (from graph) = 1600ºC
2. T min (from graph) = 500ºC
3. STRESSES:

i. Along x-axis: Tensile = 115 MPa; Compressive = 980 MPa

ii. Along y-axis: Tensile = 575 MPa; Compressive = 615MPa

iii. Along z-axis: Tensile = 12 MPa; Compressive = 60 MPa

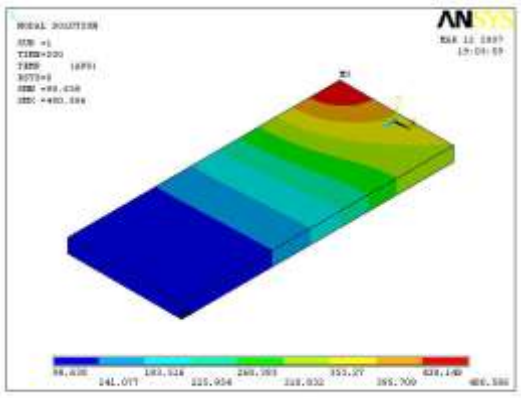

Fig.10: Temperature Distribution In The Plate

The above figure shows the distribution of temperature in the plate. Here heat flux is applied where the electrode initially comes in contact with the metal plate. Hence maximum temperature 480.586 ºC is obtained at that contact. Variation of colors represents the variation of temperature along the plate. The different values of the temperature (in centigrade) are shown in the above figure.

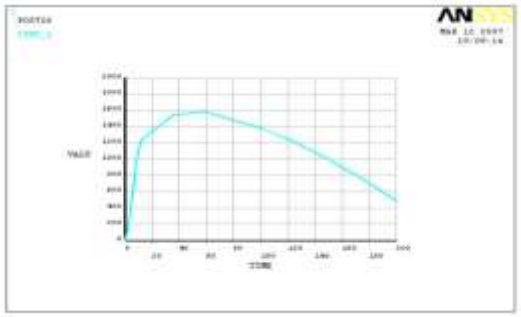

Fig.11: Temperature – Time Distribution Curve

The above graph is plotted between Temperature and Time. Time is taken on x-axis and Temperature is taken on y-axis. Due to the application of heat flux (during welding), the temperature increases up to1600ºC in a time interval of 0-40seconds. The metal plate begins to cool (after welding), due to which the temperature of the metal plate drops down to 500ºC in a time interval of 40-200seconds.

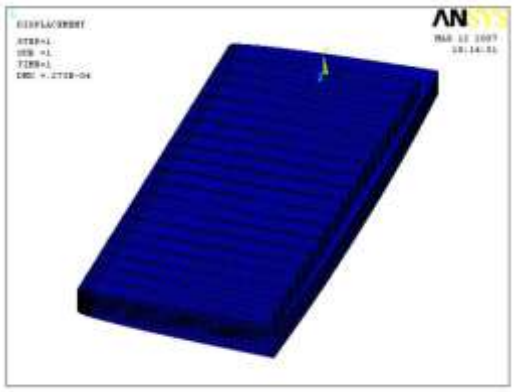

Fig.12: Deformed And Undeformed Shape Of The Plate

The figure illustrates the deformed and undeformed shaped of the metal plate after static analysis. The maximum value of deflection is found to be 2.73 x $10^{-5}$ meters.

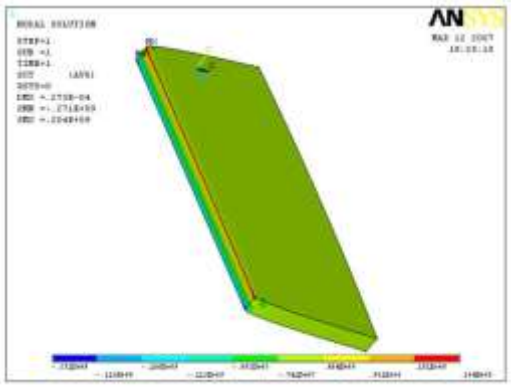

Fig.13: Shear In The XY-Plane

The figure illustrates the variation of shear stress in the XY-plane. X-axis is along the length of the plate i.e., 0.048 m. Y-axis is along the thickness of the plate i.e., 0.006 m. The value of tensile shear stress is found to be 204 MPa. The value of compressive shear stress is found to be 271 MPa. Variation of colors represents the variation of shear stress in the plate. The different values of shear stress (in MPa) are shown in the above figure.

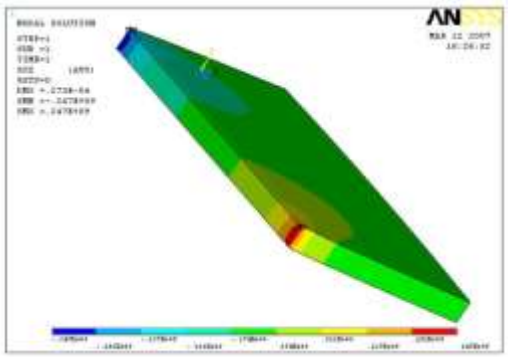

Fig.14: Shear In The XZ-Plane

The figure illustrates the variation of shear stress in the XZ-plane. X-axis is along the length of the plate i.e., 0.048 m. Z-axis is along the breadth of the plate i.e., 0.115 m. The value of tensive shear stress is found to be 247 MPa. The value of compressive shear stress is found to be 247 MPa. Variation of colors represents the variation of shear stress in the plate. The different values of shear stress (in MPa) are shown in the above figure.

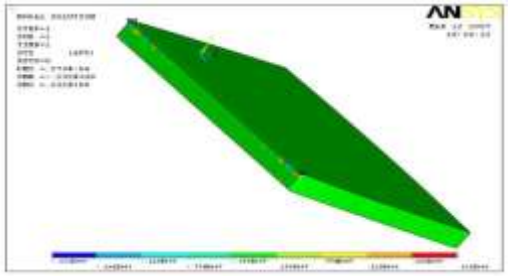

Fig.15: Shear In The YZ-Plane

The figure illustrates the variation of shear stress in YZ-plane. Y-axis is along the thickness of the plate i.e., 0.006 m. Z-axis is along the breadth of the plate i.e., 0.115 m. The value of tensile stress is found to be 23.2 MPa. The value of compressive stress is found to be 23.2 MPa. Variation of colors represents the variation of shear stress in the plate. The different values of shear stress (in MPa) are shown in the above figure.

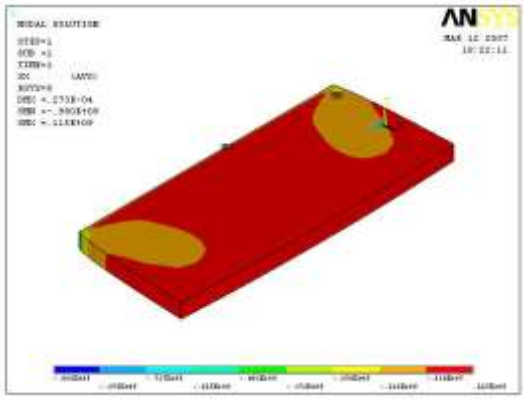

Fig.16: Stress In The X-Axis

The figure illustrates the variation of stress along the X-axis. The value of tensile stress is found to be 115 MPa. The value of compressive stress is found to be 980 MPa. Variation of colors represents the variation of stress in the plate. The different values of stress (in MPa) are shown in the above figure.

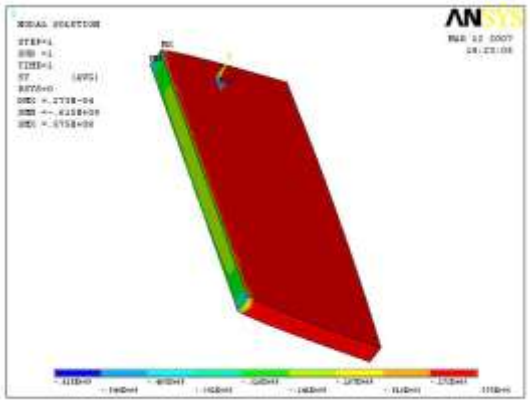

Fig.17: Stress In The Y-Axis

The above figure illustrates the variation of stress along the Y-axis. The value of tensile stress is found to be 57.5 MPa. The value of compressive stress is found to be 615 MPa. Variation of colors represents the variation of stress in the plate. The different values of stress (in MPa) are shown in the above figure.

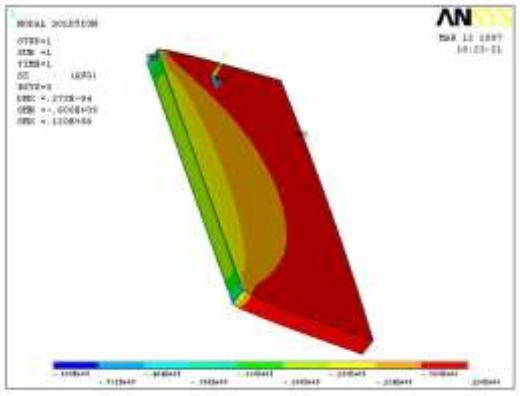

Fig.18: Stress in the Z-Axis

The above figure illustrates the variation of stress along Z-axis. The value of tensile stress is found to be 12 MPa. The value of compressive stress is found to be 600 MPa. Variation of colors represents the variation of stress in the plate. The different values of stress (in MPa) are shown in the above figure.

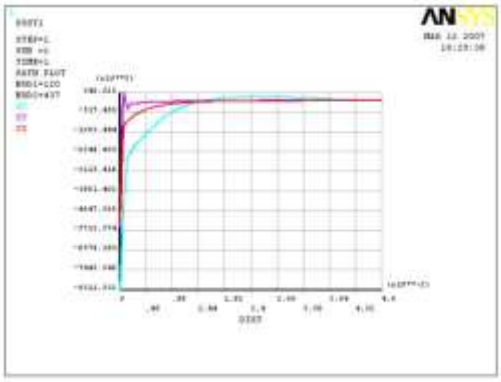

Fig.19: Graph of Stress For The Nodes Selected Along The Length Of The Plate (X-Axis)

The above figure is plotted between the stress and the nodal distance, for the nodes selected along the length of the plate. Here the nodal distance is taken on the X-axis and the stress is taken on the Y-axis. From this figure we observe that the value of stress, along the x, y and z-axis for the nodes selected along the length of the plate, increases up to a certain nodal distance and then the graph obtained is constant as shown in the figure.

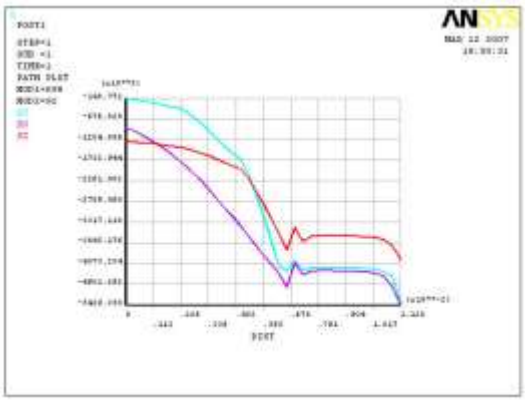

Fig.20: Stress Along The Thickness Of The Plate

The above figure is plotted between the stress and the nodal distance, for the nodes selected along the thickness of the plate. Here the nodal distance is taken on the X-axis and the stress is taken on the Y-axis. From this figure we observe that the value of stress, along the x, y and z-axis for the nodes selected along the thickness of the plate decreases. As we move down along the thickness of the plate the stress value decreases which is due to the decrease of the intensity of the heat flux on the selected nodes.

## CONCLUSION

By conducting experiment with weld parameters the heat flux is calculated and is used as input for the finite element analysis in butt-welding of plates. Heat flux value is $8.8*10^6$ J/m². A transient non-linear thermal analysis is carried out with 3D hexahedron elements to estimate the temperature variation of butt weld of the plates. Maximum temperature observed was 1600°C. Coupled field analysis is carried out to estimate the residual stresses. The maximum induced stress observed is 980 MPa.

## REFERENCES

1) ANSYS Users Manual, Revision 9.0, 2004.
2) American Welding Society, Structural Welding Code Steel-Steel, 1996.
3) Bonifaz E., "Finite Element Analysis of Het Flow in Single-Pass Arc Welds", Welding Research Supplement, May 2000, p121-125.
4) Brown S., and Song H., "Implications of Three-Dimensional Numerical Simulations of welding of large structures", welding Journal, Feb.1992, p55-62.
5) Brown S., and Song H., "Finite Element Simulation Of Welding of large structures", Journal of Engineering for Industry, Vol. 144, 1992, p441-451.
6) Frewin M., and Scott D., "Finite Element Model of Pulsed Laser Welding", Welding Research Supplement, Jan 1999, p 15-22.
7) Friedman E., "Thermo mechanical Analysis of welding process using the finite element method", Transaction of the ASME, 1975, p206 – 213.
8) Goldak J., Bibby M., Moore J., House R., and Patel B., "Computer Modeling Heat Flow in Welds"., Metallurgical Transaction B, Vol.17B, 1986, p587-600.
9) Goldak J., Chakravarthi A., and Bibby M., "A New Finite Element Model for Welding heat sources", Metallurgical Transaction B., Vol. 15B., 1984, p229-305.
10) Harwig D., Longenecker D., and Cruz J., "Effects of Welding Parameters and Electrode Atmospheric Exposure on the Diffusible Hydrogen content of Gas Shielded Flux Cored Arc Welds", Welding Research Supplement, Sept. 1999, p314-321.